

## MIXED MODE INTERFACE TOUGHNESS OF METAL / CERAMIC JOINTS

YUEGUANG WEI, JOHN W. HUTCHINSON

Division of Applied Sciences, Harvard University, Cambridge, MA 02138

### ABSTRACT

A mechanics study of the interface toughness of joints comprised of ceramic substrates joined by a thin ductile metal layer is carried out for arbitrary combinations of mode I and mode II loading. The crack lies on one of the metal/ceramic interfaces, and the mechanism of separation at the crack tip is assumed to be atomic decohesion. The SSV model proposed by Suo, Shih and Varias is invoked. This model employs a very narrow elastic strip imposed between the substrate and the ductile layer to model the expected higher hardness of material subject to high strain gradients and possible dislocation-free zone in the immediate vicinity of the crack tip. The criterion for crack advance is the requirement that energy release rate at the crack tip in this narrow elastic strip be the atomistic work of fracture. The contribution of plastic dissipation in the metal layer to the total work of fracture is computed as a function of the thickness and yield strength of the layer and of the relative amount of mode II to mode I. Ductile joints display exceptionally strong thickness and mixed mode dependencies.

### INTRODUCTION

Plastic dissipation at the tip of a crack constitutes a major fraction of the total work of fracture for many ductile structural metals and tough metal/ceramic interfaces. A quantitative understanding of interface toughness is just beginning to emerge [1,2]. Recent experiments on the toughness of metal ceramic interfaces [3-5] have helped to elucidate the relationship between the total work of fracture and the work of the fracture process. For interfaces which fail by an atomic decohesion mechanism, the total work of fracture can be hundreds of times the atomistic work of separation. Nevertheless, the atomistic work of separation sets the magnitude of the contribution from plastic dissipation, and small changes in the former can produce huge changes in the later. This exceptional nonlinear magnification has been recently demonstrated experimentally for a niobium/sapphire interface [5].

Mechanics models of the toughness of structural metals and metal/ceramic interfaces must be divided into at least two classes: those which apply to the ductile fracture process of void growth and coalescence, and those for which the atomic separation is the fracture process. The important distinction between two classes arises because of the widely different scales of the fracture processes. Void growth and coalescence takes place on a scale ranging typically from ten to a hundred microns. Conventional continuum plasticity theory is sufficiently accurate at this scale to connect the region where the loads are applied down to the crack tip where the fracture process occurs. Models [1,2,6] which embed a traction-separation relation characterizing the fracture process within a elastic-plastic continuum representation of the solid are capable of capturing the most important features of interaction between fracture process and plastic deformation. By contrast, conventional plasticity theory cannot be used at the very small scales bridging down to the tip when atomic separation is the fracture process. According to continuum plasticity crack solutions, the maximum stresses which can be attained in the vicinity of a crack tip are never more than about five times the tensile flow stress of the metal. Such levels are generally well below the stresses needed to bring about atomic separation of a strong interface. The problem of bridging from the macroscopic level down to the atomistic level at the crack tip through a plastic zone constitutes a major challenge.

In this paper, attention is directed to metal/ceramic interfaces which fail by atomic separation. The problem just alluded to will be side-stepped with a model proposed by Suo, Shih and Varias [7], which will hereafter be designated as the SSV model. This model has been proposed for metals containing at least moderate densities of pre-existing dislocations such that plastic deformation is associated with motion of these dislocations. It is assumed that no dislocations are emitted from the crack tip such that the tip remains atomistically sharp. The

essential modeling step is the imposition of an elastic strip of thickness  $t$  between the interface and the plastically deforming metal layer, as shown in Fig. 1. In a crude way, the elastic strip is intended to: (i) account for the high flow stress of metal which is expected to develop in the vicinity tip where strain gradients are very large, and (ii) represent any dislocation-free region at the tip. An elaboration on the SSV model [8] proposes a self-consistent way to identify  $t$  by matching the dislocation density and effective flow stress a distance  $t$  from the tip. In the present paper, the thickness of the elastic strip  $t$  is regarded as a parameter in the model whose value, for example, can be chosen to fit one set of experimental data.

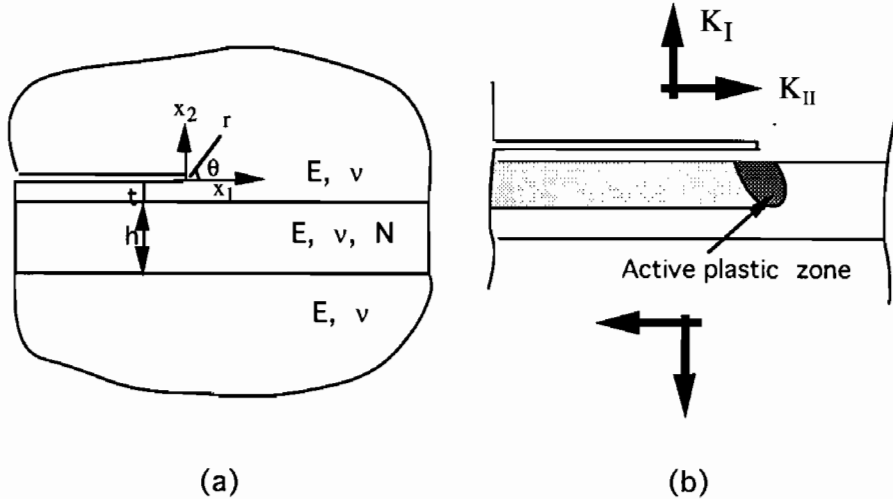


Fig.1 The joint system subjected to mixed mode K-field at remote boundary

Specifically, we model the plane strain system with a thin metal layer sandwiched between two ceramic substrates. A long crack lies along one of the interfaces. As depicted in Fig. 1, the crack is loaded by combinations of the mode I and mode II stress intensity factors,  $K_I$  and  $K_{II}$ . The tensile yield stress of the metal is  $\sigma_Y$  and its strain hardening exponent is  $N$ . To limit the number of material parameters in the study, the substrates and metal layer are assigned the same Young's modulus  $E$  and Poisson's ratio  $\nu$ . The object of the study is to predict the total work of fracture  $\Gamma_{ss}$  for the steady-state propagation of the crack down the interface in terms of the following parameters of the model: the atomistic work of separation  $\Gamma_0$ , the relative amount of mode II to mode I, as measured by  $\psi = \tan^{-1}(K_{II}/K_I)$ , the thickness of the metal layer  $h$  and its yield stress and hardening exponent,  $\sigma_Y$  and  $N$ , and  $E$  and  $\nu$ . The thickness  $t$  of the thin metal strip imposed between interface and the elastic-plastic layer is taken to be small compared to the metal layer thickness  $h$ .

#### FORMULATION OF THE STEADY-STATE CRACK GROWTH PROBLEM

Each ceramic substrate in Fig. 1 is assumed to be semi-infinite. The remote loading is specified by the mode I and II stress intensity fields:

$$\sigma_{ij} = \frac{K}{\sqrt{2\pi r}} \left[ \bar{\sigma}_{ij}^I(\theta) \cos(\psi) + \bar{\sigma}_{ij}^{II}(\theta) \sin(\psi) \right] \quad (r \rightarrow \infty) \quad (1)$$

$$\psi = \tan^{-1}(K_{II}/K_I), \quad K = [K_I^2 + K_{II}^2]^{1/2}$$

The functions depending on  $\theta$  can be found in any text book on fracture. The remote loading is characterized by  $K_I$  and  $K_{II}$  or, equivalently, by  $G$  and  $\psi$ , where Irwin's result for the energy release rate is

$$G = \frac{(1-\nu^2)}{E} K^2 = \frac{(1-\nu^2)}{E} [K_I^2 + K_{II}^2] \quad (2)$$

This quantity is interpreted as the remote, or applied, energy release rate. It will be identified with the total work of fracture for steady-state growth,  $\Gamma_{ss}$ .

As the crack tip is fully surrounded by elastic material, it is characterized by local stress intensity factors,  $K_I^{tip}$  and  $K_{II}^{tip}$ . Alternatively the tip deformation can be characterized by  $G_{tip}$  and  $\psi_{tip}$ , where

$$G_{tip} = \frac{(1-\nu^2)}{E} [K_I^{tip2} + K_{II}^{tip2}] \quad \text{and} \quad \psi_{tip} = \tan^{-1}(K_{II} / K_I) \quad (3)$$

These quantities will be computed. In the application of the crack solution,  $G_{tip}$  will be identified with the atomistic work of fracture  $\Gamma_0$ .

The tensile stress-strain curve of the metal in the layer is taken to be

$$\begin{aligned} \epsilon &= \frac{\sigma}{E} & \sigma < \sigma_Y \\ &= \frac{\sigma_Y}{E} \left( \frac{\sigma}{\sigma_Y} \right)^{1/N} & \sigma > \sigma_Y \end{aligned} \quad (4)$$

This relation is generalized to multi-axial stress states by  $J_2$  flow theory for small strain incremental plasticity (von Mises theory). For plastic loading, increments in stress and strain are related by

$$\dot{\epsilon}_{ij} = \frac{1+\nu}{E} \dot{\sigma}_{ij} - \frac{\nu}{E} \dot{\sigma}_{kk} \delta_{ij} + \frac{3\dot{\sigma}_e}{2\sigma_e} \left[ \frac{1}{E_t(\sigma_e)} - \frac{1}{E} \right] s_{ij} \quad (5)$$

where  $s_{ij}$  is the stress deviator,  $\sigma_e = \sqrt{3s_{ij}s_{ij}/2}$  and  $E_t$  is the tangent modulus of the tensile stress-strain curve at  $\sigma_e$  from (4).

The emphasis here is on steady-state growth wherein the crack has advanced sufficiently far from initiation such that stresses and strains no longer change from the vantage point of an observer translating with the crack tip. The crack problem is posed for steady-state crack growth under constant  $G$  and  $\psi$ . A zone of active plasticity moves with the tip, and a wake of plastically deformed, but elastically unloaded, material extends behind the tip, as depicted in Fig. 1. The steady-state condition for any quantity such as a Cartesian component of incremental stress is

$$\dot{\sigma}_{ij} = -\dot{a} \frac{\partial \sigma_{ij}}{\partial x_1} \quad (6)$$

where the crack is advancing in the  $x_1$  direction and  $\dot{a}$  is the increment of crack advance. A numerical method [9] which employs iteration to satisfy conditions (6) is used to directly obtain the steady-state solution. A similar method was employed in [7] and [8]. A finite element procedure with a grid especially designed to cope with the steady-state wake has been used to carry out the calculations, as will be discussed further in the next section.

The main results of interest from the solution are the functional relations between the local crack tip fields, as characterized by  $G_{tip}$  and  $\psi_{tip}$ , and the corresponding applied quantities,  $G$  and  $\psi$ . The non-dimensional forms of these relations are

$$\frac{G}{G_{tip}} = f_1[\psi, \bar{h}, \bar{l}, N, \sigma_Y / E, \nu] \quad \text{and} \quad \psi_{tip} = f_2[\psi, \bar{h}, \bar{l}, N, \sigma_Y / E, \nu] \quad (7)$$

where the two dimensionless thickness quantities are

$$\bar{h} = \frac{h}{R_0} \text{ and } \bar{t} = \frac{t}{R_0} \text{ where } R_0 = \frac{EG_{tip}}{3\pi(1-\nu^2)\sigma_Y^2} \quad (8)$$

The reference length,  $R_0$ , can be regarded as an estimate of the small scale yielding plastic zone size in plane strain for a crack loaded by  $G_{tip}$ . It will be seen to serve as a basic material length scale against which to gage whether the metal layer is thick or thin. In the limit when  $\bar{h}$  is very small, plasticity is essentially eliminated and  $G_{tip}$  and  $\psi_{tip}$  approach their applied counterparts,  $G$  and  $\psi$ . When plastic dissipation is not negligible, the steady-state work balance is precisely

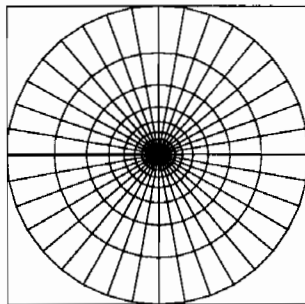
$$G = G_{tip} + G_{plastic} \quad (9)$$

where  $G_{plastic}$  denotes the plastic dissipation rate (energy per unit length of crack edge per unit length of crack advance). Thus the steady-state model permits a clear-cut partitioning of the work of crack advance into plastic dissipation and the portion available for the local fracture process,  $G_{tip}$ .

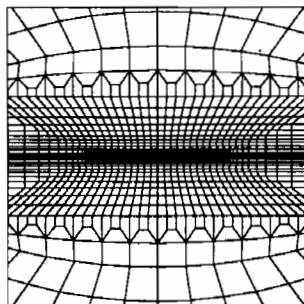
In applying the solution to establish the relation of the total work of fracture for steady-state crack advance along the joint,  $\Gamma_{ss}$ , to the atomistic work of separation of the interface,  $\Gamma_0$ ,  $\Gamma_{ss}$  is identified with  $G$  and  $\Gamma_0$  with  $G_{tip}$ . Thus, results will be presented for the ratio  $\Gamma_{ss}/\Gamma_0$ , reflecting the magnification of toughness due to plastic dissipation. The nondimensional thickness quantities are still defined in (8), but with  $R_0$  evaluated using  $G_{tip}=\Gamma_0$ .

## NUMERICAL METHOD

As described in [9], the steady-state solution procedure requires stress histories to be integrated along lines parallel to the  $x_1$  axis within the active plastic zone and the wake. This is most effectively implemented in a finite element framework if the plastic zone and wake lie within a horizontal grid whose elements at any distance above the crack line all have the same height in the  $x_2$  direction. The grid used in the present work is shown in Fig. 2. The horizontal mesh near the tip which contains the metal layer transitions to a radial mesh in the outer field. Traction obtained from (1) are prescribed on a circular boundary of radius  $R$ . In all the numerical results presented below, the computations have been performed with  $R/R_0=1012$ . This choice ensures that layer thickness and the plastic zone extent ahead of the tip will always be small compared to  $R$  in the examples considered here. Four-noded quadrilateral elements were employed and four Gauss points are used for integration. A mesh with 3664 elements was used in all the calculations reported below.



(a) Far field mesh



(b) Near tip mesh

Fig.2 Finite element mesh

The local energy release rate,  $G_{tip}$ , was computed using the J-integral such that the contour below the crack line was chosen to lie within the thin elastic strip, i.e.  $x_2 > -t$ , ensuring path-independence. The local measure of mode mix,  $\psi_{tip}$ , was identified with  $\tan^{-1}(\sigma_{12}/\sigma_{22})$  as evaluated on  $x_2=0$  just ahead of the tip.

## NUMERICAL RESULTS

All the dimensionless variables in (7) except  $\sigma_Y/E$  and  $\nu$  are important in determining  $\Gamma_{ss}/\Gamma_0$ . Numerical results will now be presented which reveal the main trends. Plots of  $\Gamma_{ss}/\Gamma_0$  as a function of  $\bar{h}$  are given in Fig. 3 for an applied mode I loading,  $\psi=0$ , for two choices of  $\bar{t}$  and three values of the strain hardening exponent  $N$ . For dimensionless metal layer thicknesses  $\bar{h}$  above a certain level (between 2 and 4 for the examples in Fig. 3),  $\Gamma_{ss}/\Gamma_0$  becomes independent of layer thickness. For values of  $\bar{h}$  above this level the plastic zone does not spread all the way across the layer to the other substrate, and a further increase of the layer thickness does not alter the plastic dissipation. The layer and the substrates have the same elastic properties in this example, and thus the limiting value of  $\Gamma_{ss}/\Gamma_0$  for large  $\bar{h}$  represents the small scale yielding toughness enhancement for the metal/ceramic interface. At the other limit, as  $\bar{h}$  approaches zero, the amount of metal deforming plastically becomes unimportant and the total work of fracture approaches  $\Gamma_0$ . The qualitative features seen in Fig. 3 are similar to those predicted by the embedded fracture process model [1,2].

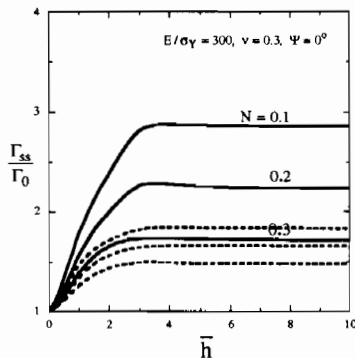


Fig.3 Variation of toughness with ductile layer thickness for different  $N$ . Solid lines correspond to  $\bar{t}=0.15$ , and dashed lines to  $\bar{t}=0.25$ .

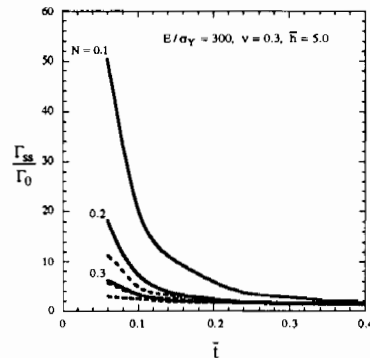


Fig.4 The variation of toughness with elastic strip thickness. Solid lines stand for  $\psi=90^\circ$ , and dashed lines for  $\psi=0^\circ$ .

The dimensionless parameter  $\bar{t}$  characterizing the thickness of the plasticity-free elastic strip in the SSV model is a critical intrinsic parameter in establishing  $\Gamma_{ss}/\Gamma_0$ . Curves displaying this ratio as a function of  $\bar{t}$  for mode I ( $\psi=0$ ) and mode II ( $\psi=90^\circ$ ) are shown in Fig. 4 for several values of  $N$ . When  $\bar{t}$  exceeds a value of roughly 1/4, there is little plasticity enhancement of toughness. The elastic strip is then sufficiently thick that it eliminates most of the crack tip shielding due to plastic deformation. For values of  $\bar{t}$  less than 1/10, the toughness enhancement becomes significant. In this range, shielding is a strong function of  $\bar{t}$ . One approach to applying the SSV model is to regard  $\bar{t}$  as a parameter to be chosen to fit one set of experimental data for a given interface. Alternatively, and more fundamentally,  $\bar{t}$  can be assigned its value using an approach such as that suggested in [8] which attempts to estimate the width of the plasticity-free region from first principles. Either way, the value of  $\bar{t}$  is associated with the interface and must be regarded as being independent of the metal layer thickness, the mode mixity, and other

extrinsic factors, such as residual stress in the metal layer, which are not considered in this paper. The value of the model rests in the fact that once  $\bar{\Gamma}$  has been set, the dependence of  $\Gamma_{ss}/\Gamma_0$  on the extrinsic factors can be computed. There is a correspondence discussed in [2] between the parameter  $\bar{\Gamma}$  of the SSV model and the ratio of the peak separation stress to the yield stress,  $\hat{\sigma}/\sigma_Y$ , of the embedded fracture process zone model. For corresponding behaviors, the smaller is  $\bar{\Gamma}$  the larger is  $\hat{\sigma}/\sigma_Y$ .

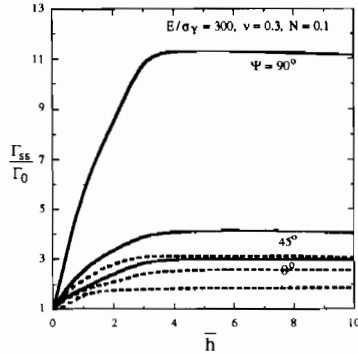


Fig. 5 Variation of toughness with ductile layer thickness for different  $\Psi$ . Solid lines stand for  $\bar{t}=0.15$ , and dashed lines for  $\bar{t}=0.25$ .

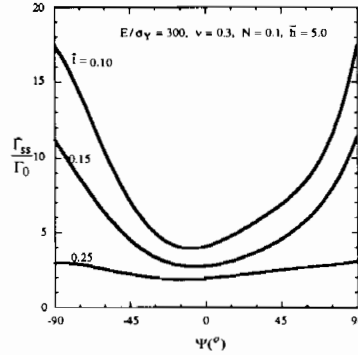


Fig. 6 The curves of toughness with applied loading mixity.

The effect of mixed mode loading is shown in Fig. 5, where plots are displayed for three values of the applied mode mixity measure  $\psi$ . For pure mode II with  $\psi=90^\circ$ , the crack along the interface remains open to the tip, as will be discussed below. Fig. 6 displays the plots of  $\Gamma_{ss}/\Gamma_0$  as a function of  $\psi$  for three values of  $\bar{t}$ , all with  $\bar{h}=5$  and  $N=0.1$ . As can be seen from the curves in Fig. 5, the dimensionless layer thickness  $\bar{h}=5$  is sufficiently large such that the mode dependence in Fig. 6 corresponds to the asymptotic limit for "thick" metal layers. Here, again, the trends are remarkably similar to the trends of toughness on mixed mode loading predicted by the embedded

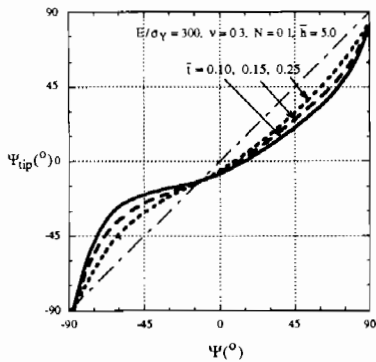


Fig. 7 Relations of applied loading mixity with crack tip mixity for three different elastic strip thickness.

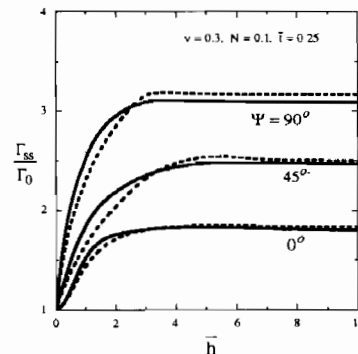


Fig. 8 Effect of yielding strain on the toughness. Solid lines stand for  $E/\sigma_Y=1000$ , and dashed lines for  $E/\sigma_Y=50$ .

fracture process model [1]. The lowest total work of fracture  $\Gamma_{ss}$  is attained for near mode I loadings. Large enhancements of toughness arise for loadings which have a major component of mode II. Of course, these enhancements are lost when the layer thicknesses are small ( $\bar{h} \ll 1$  in Fig. 3). Companion plots to those in Fig. 6 showing the relation of the local mode mixity  $\psi_{tip}$  to the applied mode mixity  $\psi$  are given in Fig. 7. The asymmetry in the relation is due to the fact that the metal layer lies below the plane of the cracked interface. Note that pure mode I at the local level corresponds roughly to  $\psi=15^\circ$  at the applied level. The crack tip is open under  $\psi=90^\circ$ , but is closed at values of  $\psi$  more negative than about  $-85^\circ$ . There is a range of applied mixed mode loadings  $\psi$ , from roughly  $-45^\circ$  to  $30^\circ$ , over which the local mode mixity is only weakly dependent on the applied mode mixity with  $\psi_{tip} \approx -15^\circ$ .

For completeness, curves displaying the effect of two choices of  $\sigma_Y/E$  are shown in Fig. 8. The effect of this parameter is very small. Note, however, that  $\sigma_Y$  has a strong influence on the toughening enhancement through  $\bar{h}$  and  $\bar{l}$  by virtue of their dependence on  $R_0$ . Calculations with different values of Poisson's ratio  $\nu$  show that this parameter also has a very weak effect on  $\Gamma_{ss}/\Gamma_0$ .

## DISCUSSION

The SSV model predicts a strong dependence of the interface toughness on the relative amount of mode II to mode I applied to the joint when plastic dissipation makes a major contribution to the macroscopic toughness. This effect is due to the more effective crack tip shielding by plastic deformation when the loading has a large component of mode II. The version of the SSV model invoked here assumes that the atomistic work of fracture  $\Gamma_0$  is independent of the local crack tip mixity,  $\psi_{tip}$ . Any local dependence on  $\psi_{tip}$  would be further magnified at the macroscopic level. Qualitatively, the mode dependence of the SSV model is similar to that displayed by the embedded fracture process zone model [1]. Both models also display a similar trend of joint toughness with the thickness of the metal layer. When the thickness of the metal layer becomes comparable to the characteristic plastic zone size,  $R_0$ , plastic dissipation is reduced. The plasticity contribution to the total work of fracture becomes nearly inconsequential for layer thicknesses below about  $R_0/4$ .

As discussed in the Introduction, the imposition of the thin elastic strip of thickness  $t$  between the interface and the metal layer in the SSV model is a device for circumventing the limitations of conventional plasticity at scales below about several microns. In this spirit,  $t$  can be regarded as a parameter in the model to be chosen to fit one set of experimental data for a given interface. More rigorous models for bridging down to the crack tip will require a plasticity theory capable of characterizing behavior at the micron to sub-micron scale when large strain gradients are present. The following numerical example illustrates the inconsistency inherent in applying the SSV model to a metal/ceramic interface undergoing atomic separation. Take the following representative values for the interface system:  $E=200\text{GPa}$ ,  $\sigma_Y=200\text{MPa}$ , and  $\Gamma_0=1\text{Jm}^{-2}$ . Then, by (8),  $R_0=0.5\mu\text{m}$ . From the numerical results (cf. Fig. 4), values of  $\bar{l}=t/R_0$  needed to give rise to significant levels of plastic dissipation must be less than about 0.2. Thus, the thickness of the plasticity-free elastic strip must satisfy  $t < 0.1\mu\text{m}$ . While such values are reasonable, it is not reasonable to expect conventional plasticity will remain valid down to the strip. In other words, even with the introduction of the elastic strip, there remains a significant domain of the model within which the rationale for using conventional plasticity is highly questionable.

## ACKNOWLEDGMENT

This work was supported in part by the Natural Science Foundation under Grants MSS-92-02141 and DMR-94-00396, in part by Young Scientist Award for Y.W. from the Chinese Academy of Sciences, and by the Division of Applied Sciences, Harvard University.

## REFERENCES

1. V. Tvergaard and J. W. Hutchinson, *J. Mech. Phys. Solids*, **41**, p.1119(1993).
2. V. Tvergaard and J. W. Hutchinson, *Phil. Mag.*, **70**, p.641(1994).
3. I. E. Reimanis, B. J. Dalgleish, M. Brahy, M. Ruhle, M. and A. G. Evans, *Acta Metall. Mater.*, **38**, p.2645(1990).
4. I. E. Reimanis, B. J. Dalgleish, and A. G. Evans, *Acta Metall. Mater.*, **39**, p.3133(1991).
5. G. Elssner, D. Korn and M. Ruhle, *Scripta Metallurgica et Materialia*, **31**, p.1037(1994).
6. A. Needleman, *J. Appl. Mech.*, **54**, p.525(1987).
7. Z. Suo, C. F. Shih and A. G. Varias, *Acta Metall. Mater.*, **41**, p.1551(1993).
8. G. E. Beltz, J. R. Rice, C. F. Shih and L. Xia, A Self-Consistent Model for Cleavage in the Presence of Plastic Flow, Submitted to *Acta Metall. Mater.*, (1995).
9. R. H. Dean and J. W. Hutchinson, Quasi-static steady crack growth in small-scale yielding, Fracture Mechanics: Twelfth Conference, ASTM STP700, p.383(1980), Philadelphia, PA.